# Growth mode and magnetic behavior of thin Fe films on $Cu_3Au(001)$ studied by low-energy electron diffraction and spin-resolved electron spectroscopies

R. Rochow,* C. Carbone, Th. Dodt,† F. P. Johnen, and E. Kisker*
*Institut für Festkörperforschung der Kernforschungsanlage Jülich, Postfach 1913, D-5170 Jülich 1, Germany*
(Received 17 July 1989; revised manuscript received 16 October 1989)

The structure and magnetic behavior of ultrathin Fe films on $Cu_3Au(001)$ have been examined. By low-energy electron diffraction (LEED) and Auger measurements it is shown that films up to a thickness of 7 monolayers (ML) deposited at room temperature grow pseudomorphically as face-centered-cubic Fe(001) with the $Cu_3Au$ lattice parameter of 3.75 Å parallel to the surface. The films grow layer by layer. The magnetism of the fcc Fe films has been investigated by spin-polarized secondary-electron spectroscopy as a function of film thickness. The spin-polarization component parallel to the film plane is zero for films thinner than 3.6 ML. The nonzero spin polarization for films thicker than 3.6 ML indicates the existence of remanent magnetization parallel to the surface at room temperature. Spin-resolved photoelectron spectroscopy with synchrotron radiation has been used to study the electronic and magnetic structure of the films. The high spin polarization $P > 50\%$ of the photoelectrons clearly demonstrates the ferromagnetism of $\gamma$-Fe with a lattice constant of 3.75 Å. The spin-resolved energy distribution curves (SREDC's) may be understood according to the spin-resolved band-structure calculations of Bagayoko and Callaway [Phys. Rev. B **28**, 5419 (1983)]. The results indicate that in contrast to $\alpha$-Fe, $\gamma$-Fe with a lattice parameter of 3.75 Å is a strong ferromagnet.

## I. INTRODUCTION AND MOTIVATION

At room temperature, the stable structure of Fe is the body-centered-cubic $\alpha$-Fe structure, while above 1183 K face-centered-cubic $\gamma$-Fe becomes the stable state.[1] The magnetic properties of $\alpha$-Fe have been investigated thoroughly and are relatively well understood. In contrast, experimental results on the magnetism of $\gamma$-Fe are contradictory. To investigate the magnetic behavior of $\gamma$-Fe it is necessary to stabilize this structure at temperatures below the critical temperature for the structural phase transition in Fe. Above this temperature $\gamma$-Fe is paramagnetic with a negative Curie temperature.[2] It has been shown that the fcc structure may be stabilized in small Fe precipitates in a Cu matrix at low temperatures[3] and in Fe films on Cu surfaces.[4–6] While $\gamma$-Fe precipitates are found to be antiferromagnetic[7–9] with a Neel temperature of 67 K which decreases with particle size,[8] the present results on $\gamma$-Fe films on Cu are not definite. Ferromagnetism at room temperature[10–12] as well as paramagnetism at room temperature and a phase transition to antiferromagnetic behavior at low temperature[13–16] was reported for $\gamma$-Fe on different Cu surfaces. In photoemission and surface magneto-optical Kerr-effect experiments an easy axis of magnetization perpendicular to the film plane for films thinner than 6 monolayers (ML) was found,[17,18] turning into the plane for thicker films.[18] Evidence for a strong dependence of the magnetic behavior on the growth conditions, especially the sample temperature during evaporation, was reported in experimental and theoretical work.[19]

Calculations of Fu and Freeman[20] for two fcc Fe layers on Cu(001) predicted ferromagnetic coupling between these layers and between the Fe atoms within one layer, and an enhanced Fe moment of $2.85\mu_B$ at the surface. A strong dependence of the magnetic moment of $\gamma$-Fe on the lattice constant has been predicted.[21–28] Based on various experimental results about the behavior of the electrical resistance, thermodynamic and volumetric properties as functions of temperature and pressure, Weiss and co-workers postulated different magnetic phases at different lattice parameters.[21,22] The existence of these magnetic phases is supported by self-consistent spin-polarized band-structure calculations by different authors.[23–28] Some of these calculations show that there may be a range of coexistence of different phases for fcc Fe.[26–28] The theoretical considerations on the lattice-parameter dependence of magnetism in fcc Fe are supported by experimental investigations of Isbert and Gradmann[29] on the magnetic moment of $\gamma$-Fe(110) on Cu-Au alloys as a function of lattice parameter, which was found to be similar to that predicted by Andersen *et al.*[23,24] These results may explain the different behavior of $\gamma$-Fe precipitates and $\gamma$-Fe films on Cu by a difference in the lattice constant of the Fe. $\gamma$-Fe precipitates with a lattice parameter of 3.57 Å are clearly in the antiferromagnetic region. $\gamma$-Fe films epitaxially grown on a Cu surface exhibit an expanded lattice constant of 3.61 Å corresponding to that of the Cu matrix. This lattice parameter belongs to the critical region near the phase transition from the antiferromagnetic state to the low-spin ferromagnetic state. Therefore for Fe on Cu the results of investigations into the magnetic properties may strongly depend on details of the film preparation, as suggested by the experimental results.[19] Furthermore, the magnetic properties of thin films may be determined by magnetic anisotropies

 

which depend on temperature and film thickness, as well as by lattice distortions and defects induced by the interface.

The aim of the experiments presented here was to investigate the magnetic properties of fcc Fe with a lattice constant which clearly lies in the high-moment region as a function of film thickness. Furthermore, the electronic structure of these films should be investigated and compared to theoretical predictions on the spin-split band structure of fcc Fe with increased lattice constant. As a substrate for the films we chose $Cu_3Au$ with a lattice constant of 3.75 Å.[30] Recently pseudomorphical growth of Fe on $Cu_3Au(001)$ has been reported for the first time.[31] In these experiments pseudomorphical growth was only found for film thicknesses up to 3 ML, while we were able to grow pseudomorphical Fe films on $Cu_3Au(001)$ with thicknesses up to 7 ML. Therefore we will first present our investigation on the growth of Fe onto the $Cu_3Au$ substrate and then show our results on the magnetic and electronic structure.

## II. SAMPLE PREPARATION AND STRUCTURAL ANALYSIS

Our samples were prepared in an ultrahigh vacuum (UHV) chamber with a base pressure of $6\times10^{-11}$ mbar. The Fe films were deposited by electron-beam evaporation at $4\times10^{-9}$ mbar with evaporation rates of 0.2 Å/min and the substrate at room temperature during evaporation. Before evaporation, the $Cu_3Au(001)$ crystal was cleaned by Ne-ion bombardment, heating to a temperature of 500 °C and annealing. The cleanliness of the crystal was monitored by Auger electron spectroscopy, the surface order by low-energy electron diffraction (LEED). The deposition rate was checked by a quartz oscillator. To determine the structure of the Fe films deposited onto the $Cu_3Au$, lattice constants parallel and normal to the surface have been measured.

Lattice parameters parallel to the surface were determined by analyzing LEED patterns. Figure 1(a) shows the LEED pattern of a clean and ordered $Cu_3Au$ crystal

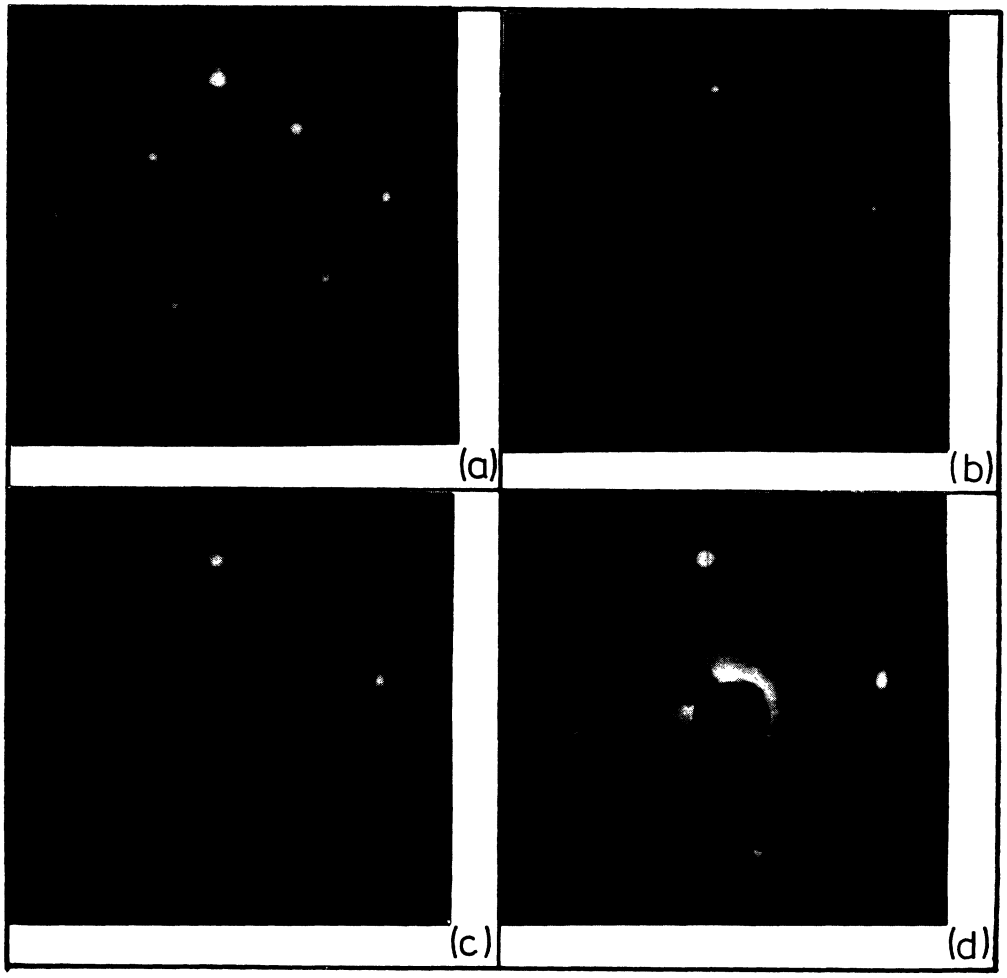


FIG. 1. (a) LEED pattern at 70 eV of a clean and ordered $Cu_3Au(001)$ surface; the four (11) spots are evident. The spots between the (11) spots are due to the superstructure of the ordered alloy. (b) LEED pattern at 70 eV of a clean $Cu_3Au$ surface at $T > 390$ °C: the superstructure spots have vanished. (c) LEED pattern at 70 eV after deposition of 5 ML of Fe: the (11) spots remained at the same position as for $Cu_3Au$. (d) LEED pattern at 55 eV after deposition of 250 ML of Fe: the four (10) spots are evident. The lattice parameter is 2.85 Å.

at an energy of 70 eV. The pattern consists of eight spots. The four outermost spots are the (11) spots, the others are due to the superstructure of the ordered alloy. They vanished by heating the sample to a temperature above the critical temperature of 390 °C for the order-disorder transition of the alloy.[1] The corresponding LEED pattern is shown in Fig. 1(b). After Fe deposition of 1 ML, the superstructure spots vanished. At the same energy the (11) spots remained at the same positions as for the $Cu_3Au$ matrix, indicating pseudomorphic growth with the same lattice constant of 3.75 Å parallel to the surface. This is shown in Fig. 1(c). As for the $Cu_3Au$, maximal intensity of the LEED spots was found at 70 eV. Fe films of 250 ML thickness and more showed maximal intensity of the LEED spots at 55 eV instead of 70 eV. This indicates that the structure of these thick films is different from the structure of the films up to 7 ML. The LEED pattern of a 250-ML film at 55 eV is shown in Fig. 1(d). For thick films the spots are interpreted as the (10) spots of the bcc Fe lattice. The lattice constant parallel to the surface calculated from the spot positions is 2.85 Å.

Lattice parameters normal to the surface were obtained by taking the intensity versus voltage dependence of the (00) LEED beam for $Cu_3Au$, Fe films on $Cu_3Au$ of various thicknesses and for bcc Fe. The experiments were performed with an polar angle $\theta$ of 10° relative to the surface normal and an azimuthal angle of 45° relative to the [100] direction of the $Cu_3Au$ substrate. The energy positions $E_n$ of the intensity maxima are given[32,33] for normal incidence

$$E_n = \frac{\hbar^2}{2m}\left[n\frac{2\pi}{a^{\perp}}\right]^2 + E_0 \ .$$

$E_0$ is the inner potential and $n$ an index for the intensity maximum considered. From the measured energy positions $E_n$, the lattice constant $a^{\perp}$ perpendicular to the surface can be calculated. For fcc Fe films on $Cu_3Au(001)$ grown with the expanded lattice constant of the $Cu_3Au$ (Ref. 30) we expect a lattice constant of about 3.75 Å perpendicular to the surface, which might be contracted due to the expansion of the lattice parameter parallel to the surface induced by the lattice mismatch between $Cu_3Au$ and $\gamma$-Fe. In contrast, bcc Fe films grown on the $Cu_3Au$ matrix with a contracted lattice constant of $3.75/\sqrt{2}$ Å and the (001) direction in the film plane rotated by 45° to the (001) direction of the $Cu_3Au$ would exhibit a lattice parameter probably expanded compared to that of the bcc Fe of 2.87 Å (Ref. 30) perpendicular to the surface due to the compressive stress in plane induced by the lattice mismatch. The I(V) curves for the LEED (00) beam of the $Cu_3Au(001)$ and Fe films of different thicknesses grown on this substrate are shown in Fig. 2. They agree well with the curves given by Lu *et al.*[31] Figure 3 gives the evaluation of these plots for $Cu_3Au$, a 5-ML film and a 250-ML film. The results for all films from 1 ML thickness to 7 ML thickness are the same as for the 5-ML film. Indices $n$ were given to each intensity maximum and its energy position $E_n$ was plotted as a function of $n^2$. The indices were chosen in such a way that the deviations of the resulting points from a straight line were minimized. From the slope of the curve, the lattice constant normal to the surface can be calculated, as can easily be seen, from the formula given above. For $Cu_3Au$ a lattice constant of 3.76 Å and an inner potential of −11.4 eV was

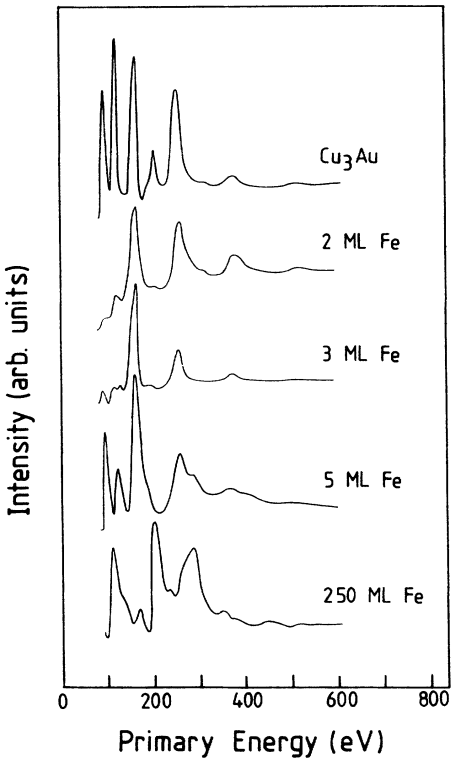


FIG. 2. Intensity vs voltage dependence of the LEED (00) beam for $Cu_3Au$ and Fe films of various thicknesses taken with a polar angle of incidence of 10° and an azimuthal angle of incidence of 45° relative to the [100] direction of the substrate: the thin-Fe films have a lattice parameter of 3.75 Å normal to the surface, which is close to the value for $Cu_3Au$. The 250-ML film exhibits a lattice constant of 2.91 Å normal to the surface, indicating bcc structure.

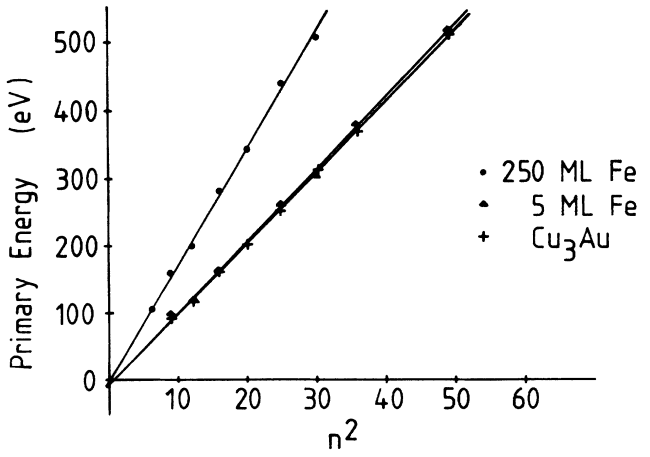


FIG. 3. Energy position $E_n$ of the intensity maxima versus an index $n^2$: the lattice constant normal to the surface can be obtained from the slope of the curve.

obtained from the data. The lattice parameter normal to the surface for the Fe films with thicknesses between 1 and 7 ML calculated from the I(V) curves are 3.75 Å. For 250- and 450-ML-thick films a lattice constant of 2.91 Å is obtained. The inner potentials obtained from these data are −8.7 eV for the thin fcc Fe films and −5.5 eV for the thick bcc Fe films.

For the clean $Cu_3Au(001)$ surface we measure a lattice constant of 3.76 Å parallel and perpendicular to the surface. This agrees within the experimental error of ±0.04 Å with the literature value of 3.75 Å. For thin Fe films up to 7 ML thickness, the lattice constants parallel and normal to the (001) surface are 3.76 and 3.75 Å, respectively. The lattice constant of the Fe film perpendicular to the film plane is slightly smaller than that of the $Cu_3Au$ substrate, as can already be seen from the steeper slope of the curve for 5 ML of Fe in Fig. 3. A decrease of the perpendicular lattice parameter would be expected for fcc Fe on $Cu_3Au$ due to the stress induced by the mismatch of about 4% between the $Cu_3Au(001)$ and the fcc Fe(001) lattice constants, which tends to stretch the Fe lattice constant in the film plane. A tetragonal distortion of the unit cell due to lattice mismatch was also reported for Fe on Cu(001).[31,19] It is possible that the difference between the lattice parameters parallel and perpendicular to the surface is even bigger than suggested by the experimental values because the errors quoted here are purely experimental. They do not take into account the limits of the kinematical model used to determine the perpendicular lattice constant for low-energy electrons. We conclude that these Fe films grow epitaxially and pseudomorphically as fcc Fe(001) onto the $Cu_3Au(001)$ surface with the $Cu_3Au$ lattice constant parallel, and a probably slightly smaller lattice constant perpendicular to the film plane.

Above a thickness of 10 ML of Fe on $Cu_3Au(001)$ the LEED pattern became worse and vanished at about 20 ML. With increasing film thickness a LEED pattern developed again. At about 100 ML it consisted of very broad spots which became sharper with increasing thickness of the overlayer.

The results for 250- and 450-ML films of Fe on $Cu_3Au$ are consistent with the value of 2.87 Å expected for bcc Fe. The measured lattice constants are 2.91 Å perpendicular and 2.85 Å parallel to the surface. The difference suggests a slight perpendicular uniaxial strain. This means that films thicker than 250 ML grow in body-centered-cubic structure onto the $Cu_3Au(001)$ with a perpendicular spacing between the planes which might be stretched due to the misfit of nearly 8% between the lattice of the substrate and that of bcc Fe leading to a compressive stress in the film plane.

The growth mode of the films was determined by Auger-electron spectroscopy. The low-energy Auger lines of Fe at 47 eV, Cu at 60 eV, and of Au at 67 eV were taken as a function of deposition time at constant deposition rate. For island free growth the Auger signal of the deposit should increase as $1-\exp(-d/D)$ and the Auger signal of the substrate should decrease as $\exp(-d/D)$.[34,35] Here $d$ is the film thickness and $D$ is the mean free path of the Auger electrons as described by Seah.[35] The Auger intensities were normalized to the sum of all three Auger amplitudes according to Ref. 34. The mean-free-path $D$ was given by Gradmann[4] to be 3 ML for the fcc Fe(111) surface. Figure 4 shows the normalized Auger signal of the Fe as a function of deposition time at a constant rate of deposition. The curve exhibits the exponential form expected for layer-by-layer growth. For each layer, the curve may be approximated by a straight line. For layer by layer growth, the ratio of gradients of adjacent lines should be a constant which is, indeed, observed within the error limits. After the deposition of 1 ML of Fe onto the $Cu_3Au$ the superstructure spots vanished. This rapid attenuation of the superstructure spots might be due to the occurrence of some intermixing at the interface for the first monolayer, as was also found by Chambers *et al.*[36] Furthermore, the photoemission spectra, which will be discussed in detail later, indicate some amount of Au segregation but no Cu segregation in agreement with the Auger spectra.

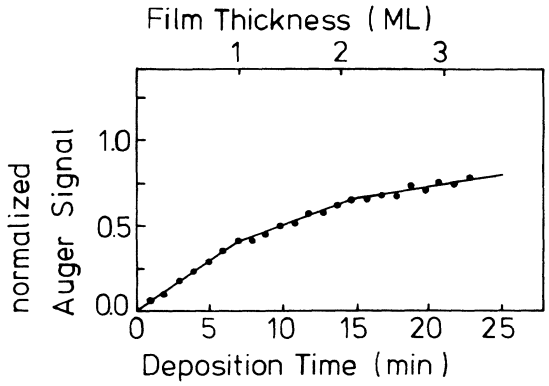


FIG. 4. Normalized Auger intensities as a function of film thickness for the 46-eV Fe Auger line.

The fact that our samples grew pseudomorphically up to 7 ML, while Lu *et al.*[31] did not find pseudomorphical growth for films thicker than 3 ML, may be explained by the different conditions during evaporation, for example, the different evaporation rates. Gradmann *et al.*[12] have shown that the growth mode of Fe onto Cu(111) depends strongly on the deposition rate and temperature. Furthermore, also for Fe/Cu different authors reported different thicknesses up to which they found pseudomorphical growth.[4,37,18] This suggests a strong dependence of the growth mode on the experimental conditions. These reasons may also be true for $Fe/Cu_3Au$.

## III. MAGNETIZATION AS A FUNCTION OF FILM THICKNESS

To test for ferromagnetism, spin-resolved electron-energy-loss experiments have been carried out. The spin polarization is defined as

$$P(E)=\frac{N^{\uparrow}(E)-N^{\downarrow}(E)}{N^{\uparrow}(E)+N^{\downarrow}(E)},$$

where $N(E)$ is the number of electrons at an electron energy $E$, and $\uparrow(\downarrow)$ refers to electrons with magnetic moments parallel (antiparallel) to the magnetization direc-

tion. Electrons of 400-eV primary energy from a commercial electron gun were inelastically scattered at the surface of the specimen. For the scattering experiments the angle of incidence was 32.5° to the surface normal, and the angle of the scattered electrons was 42.5°. To magnetize the specimen along the [110] direction a magnetic field of about 840 Oersted was applied to the target by running a current pulse of 200 A through a magnetization coil which was mounted underneath the sample. The direction of the magnetization was reversed periodically and spectra for both magnetization directions were taken alternatively to determine the apparatus asymmetry.

As a probe for long-range ferromagnetic order, secondary electrons of $E=47$ eV kinetic energy were selected by the electron energy analyzer. The spin polarization of these electrons was measured with the help of a Mott detector. Secondary electrons from a ferromagnet have been shown to be spin polarized.[38] At $E=47$ eV the spin polarization is slightly enhanced due to the superposition of the spin-polarized *MVV* Auger electrons.[38] The spin polarization was measured as a function of film thickness to detect at which film thickness spin polarization sets in.

The measured spin polarization as a function of film thickness is shown in Fig. 5. Spin polarization is first detected at a thickness of 3.6 monolayers, reaching a value of about 9% at 5.3 monolayers. The data show that there exists remanent in-plane magnetization for fcc Fe films on $Cu_3Au(001)$ thicker than 3.6 ML at room temperature. For thinner films no magnetic in-plane remanence is found. This does not mean necessarily that films thinner than 3.6 ML are not ferromagnetic. It is known that for ultrathin films the Curie temperature and the magnetic anisotropies may strongly depend on the film thickness. For samples of 1 ML of bcc Fe(110) on W(110) a Curie temperature of 210 K was found[39] by conversion electron Mössbauer spectroscopy, while 1 ML of Co on Cu(001) was found to be ferromagnetic up to 400 K by spin-polarized photoemission.[40] In both cases the Curie temperature is strongly reduced compared to the bulk value. A large reduction is also found for Co(111) and $Ni_{48}Fe_{52}(111)$ on Cu(111) by torsion magnetometry.[41] Also for $\gamma$-Fe films on Cu(001) a Curie temperature below room temperature was found for films thinner than 5 ML.[17] Therefore it cannot be excluded

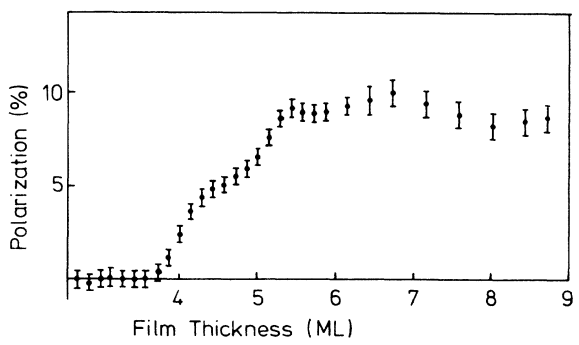


FIG. 5. Spin polarization of the 46-eV Fe Auger electrons as a function of film thickness: remanent magnetization parallel to the surface exists for films thicker than 3.6 ML.

that the Curie temperature of fcc Fe films on $Cu_3Au(001)$ thinner than 3.6 ML is below room temperature. Furthermore, a magnetic anisotropy perpendicular to the film plane as was found for $\gamma$-Fe on Cu(001) (Ref. 17) could also lead to zero spin polarization in the film plane. As the spectrometer only permits the measurement of the spin-polarization components parallel to the surface, perpendicular spin polarization was not investigated. A strong dependence of magnetic anisotropies on the film thickness has been found in many cases.[37,41,42] In our experiments the onset of spin polarization parallel to the surface appears at about the same thickness where it was found for bcc Fe(001) on Ag(001) by Jonker *et al.*[43] For bcc Fe(001) on Ag(001) at room temperature N. C. Koon *et al.*[42] showed by conversion electron Mössbauer measurements that films of 1 and 2.4 ML thickness are remanently magnetized perpendicular to the surface, while for a film of 5.5 ML thickness the remanent magnetization lies in the film plane. Also for the system studied here, fcc $Fe/Cu_3Au(001)$, strong magnetic anisotropies leading to a remanent magnetization normal to the surface might exist for films thinner than 3.6 ML. The results suggest that for $\gamma$-Fe on $Cu_3Au(001)$ the easy axis turns into the film plane at lower coverages than for $\gamma$-Fe on Cu(001), where Pescia *et al.*[17] reported a perpendicular easy axis also for 5 ML. The existence of nonzero spin polarization in the film plane at room temperature for films thicker than 3.6 ML agrees with the measurements of Isbert and Gradmann[29] on fcc Fe on $Cu_3Au(111)$, who detected ferromagnetism with high magnetic moment for lattice constants bigger than 3.65 Å. The measurements support the prediction that fcc Fe with the lattice constant of $Cu_3Au$ is ferromagnetic.[20–28]

## IV. SPIN-POLARIZED PHOTOEMISSION STUDY OF THE ELECTRONIC STRUCTURE

In Fig. 6 we present spin-integrated EDC's for clean $Cu_3Au(001)$ and for various fcc Fe films on $Cu_3Au(001)$ of different thickness taken at photon energies of 30 and 45 eV for normal emission. For normal emission the features in the spectra correspond to initial states in the $\Gamma X$ direction of the band structure. For normal emission with *s*-polarized light, only states with $\Delta_5$ symmetry are observed in the spectrum if no spin-orbit coupling exists.[44] With spin-orbit interaction, $\Delta_2$ and $\Delta_{2'}$ states are mixed into $\Delta_5$ and the resulting bands are labeled $\Delta_7$. The photoemission spectra show two groups of peaks: the peaks above 4 eV binding energy are predominantly copperlike with some gold character due to hybridization, while those below 5 eV binding energy are mostly goldlike.[44]

Fig. 6(a) shows the spin-integrated energy distribution curves taken at a photon energy of 30 eV. The $Cu_3Au$ spectrum consists of four peaks at binding energies of 3.3, 4.8, 6.0, and 6.8 eV. The peak at 3.3 eV is split and shows two shoulders at 2.3 and 3.5 eV binding energy. These peaks are due to emission from the two spin-orbit split bands with $\Delta_7$ symmetry near $\Gamma_7$ and $X_{7-}$ around 3.3 eV below $E_F$. The shoulder is due to emission from the $\Delta_7$ symmetry band from $\Gamma_{7+}$ to $X_{7-}$ near 2 eV below

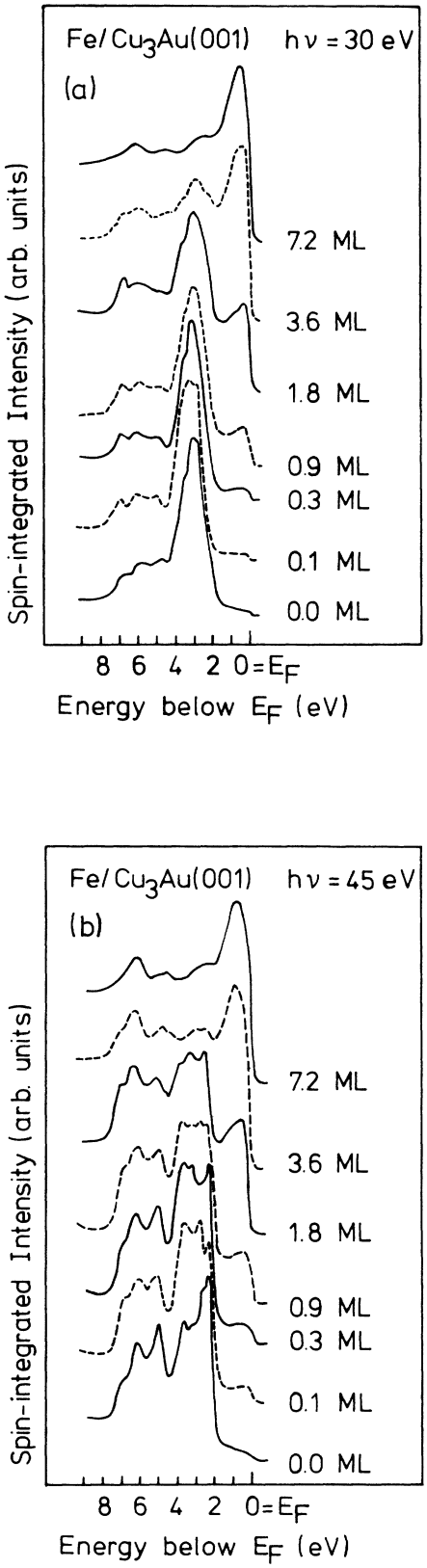


FIG. 6. Spin-integrated energy distribution curves for normal emission with *s*-polarized light from clean $Cu_3Au(001)$ and fcc Fe films on $Cu_3Au(001)$ of different thickness for photon energies of (a) 30 and (b) 45 eV.

$E_F$. Also the energy positions of the three peaks at higher binding energies correspond to emission from bands with $\Delta_7$ symmetry, those at 4.8 and 6 eV binding energy describe the emission from the spin-orbit split bands between $\Gamma_{7+}$ and $X_{7+}$, while that at 6.8 eV below $E_F$ describes emission from the band $\Gamma_{7-}$ to $X_7$.[44] Comparison of the spectrum with experimental data at 32 eV photon energy by Wang *et al.* shows good agreement between the peak positions for normal emission. For 45 eV photon energy the spectra are shown in Fig. 6(b). The peak at 2.3 eV binding energy and the features between 5 and 7 eV binding energy are dominant in agreement with the results by Wang *et al.*[44] In contrast to their spectra at 44 eV, the different features are much better resolved in our spectrum. The dominant peak is due to emission from the band of $\Delta_7$ symmetry near the $\Gamma$ point 2.5 eV below $E_F$ and near $X_7$ 2.3 eV below $E_F$; all the other peak positions are the same as for 30 eV photon energy.

With increasing film thickness of fcc Fe on the $Cu_3Au(001)$, two peaks appear which are due to photoemission from the Fe overlayer. The peak which grows strongly near the Fermi level at a binding energy of 1 eV is due to emission from the *d* bands near $\Gamma_{25}'$, $X_2$, $\Gamma_{12}$, and $X_5$. The peak at 2.5 eV binding energy in the spectrum for 7.2 ML of fcc Fe on $Cu_3Au$ is due to emission from the majority spin band $\Gamma_{25'}$ of the spin-split band structure of the ferromagnetic fcc Fe. Furthermore, we detect strong changes in the $Cu_3Au$ valence-band emission with Fe coverages as small as 0.1 ML. These Fe coverages do not change the LEED pattern which means that the surface symmetry remains the same. The observed differences in the spectra may be explained by adsorbate-induced changes in the surface potential or by surface relaxation, which can strongly influence the surface electronic structure. With increasing Fe thickness the emission from Cu 3*d* derived states (2–4 eV) decreases faster than the Au 5*d*-related emission (4–7 eV). This effect can be seen very well in the series of spectra taken at a photon energy of 30 eV. At this photon energy the Au 5*d* emission peaks are much smaller than the Cu 3*d* emission peaks in the spectrum of the clean $Cu_3Au$. After deposition of 7.2 ML of Fe onto the surface, the Cu emission has almost vanished, while the Au emission is still clearly seen. This observation may indicate that even at room temperature a limited amount of surface segregation of Au atoms occurs.

Figure 7 shows spin-resolved energy distribution curves for 5.4 ML of fcc Fe on $Cu_3Au(001)$ for normal emission and different photon energies. The spectra for majority spins are plotted with solid lines, and those for minority spins with dashed lines. It can clearly be seen that 5.4 ML of fcc-Fe on $Cu_3Au(001)$ are ferromagnetic, as the energy distribution curves are different for majority and minority spins. In addition to this we observe a spin polarization of more than 50% for fcc Fe films thicker than 4.5 ML. For normal emission from the (001) surface $\mathbf{k}^{\parallel}=0$ and $\mathbf{k}^{\perp}$ is found along $\Gamma X$ in the Brillouin zone. Therefore one has to compare the peak positions in the photoemission spectrum with the band structure of fcc Fe along $\Gamma X$, which has been calculated for a lattice

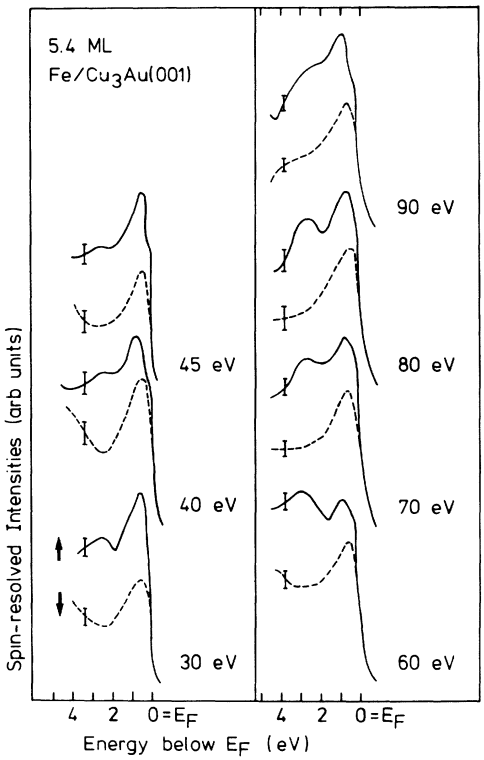


FIG. 7. Spin-resolved energy distribution curves for normal emission from 5.4 eV of fcc Fe on $Cu_3Au(001)$ for different photon energies.

constant of 7.0 a.u. by Bagayoko *et al.*[25] The majority spin energy distribution curve for 5.4 ML of fcc Fe on $Cu_3Au$ exhibits three emission features. The peak at a binding energy of 2.6 eV is due to emission from $\Gamma_{25'}^{\uparrow}$. With increasing photon energy this peak becomes broader. It shifts slightly from a binding energy of 2.6 eV at a photon energy of 30 eV to a binding energy of 2.8 eV at a photon energy of 60 eV and more. The energy position of this peak has been calculated to be 2.3 eV below the Fermi level for a lattice constant of 3.7 Å by Bagayoko *et al.*[25] Furthermore, the intensity of this peak relative to the second peak at a binding energy of 0.9 eV increases up to a photon energy of 60 eV and decreases again. The second peak 0.9 eV below $E_F$ is due to emission from the band between $\Gamma_{12}^{\uparrow}$ and $X_2^{\uparrow}$. The binding energy calculated by Bagayoko *et al.*[25] is 1.3 eV near $\Gamma_{12}^{\uparrow}$ and 0.5 eV near $X_2^{\uparrow}$. For normal emission and *s*-polarized light it should not be found in the spectrum, according to photoemission selection rules. It appears to be due to the limited angle resolution of the spectrometer. The shoulder at the low-energy side of this peak at 0.4 eV binding energy describes the emission from initial states at $X_5^{\uparrow}$. The binding energy of these states has been calculated[25] to be 0.2 eV. The existence of this peak in the photoemission spectrum means that the top of the fcc Fe *d* bands, which is found at $X_5^{\uparrow}$, lies below the Fermi level. We conclude that in contrast to $\alpha$-Fe, $\gamma$-Fe is a strong ferromagnet.

The minority spin channel exhibits one peak at a binding energy of 0.5 eV for a photon energy of 30 eV. Also this peak, which is due to emission from $\Gamma_{25'}^{\downarrow}$, shifts slightly to higher binding energy with increasing photon energy. At 60 eV photon energy it is found 0.7 eV below $E_F$. Like the majority spin emission peak from $\Gamma_{25'}^{\uparrow}$, also this peak becomes broader with increasing photon energy. The peak position is shifted by about 0.5 eV to higher binding energy compared to the calculated band structure,[25] where it appears near $E_F$. The experimentally determined exchange splitting of the *d* bands near $\Gamma_{25}'$ is 2.2 eV in the spectra, in good agreement with theoretical predictions.[25]

## V. CONCLUSION

In conclusion, we have shown by LEED and Auger electron spectroscopy that ultrathin Fe films on $Cu_3Au(001)$ grow epitaxially as fcc Fe with a lattice constant of 3.75 Å up to a thickness of 7 ML. We do not exclude a slight tetragonal distortion of the unit cell due to the stress induced in plane by the lattice mismatch of fcc Fe compared to $Cu_3Au$. Films thicker than 250 ML grow as body-centered-cubic Fe with a lattice constant of 2.91 Å perpendicular and a lattice constant of 2.85 Å parallel to the surface. fcc Fe films with a lattice constant of 3.75 Å and thicker than 3.6 ML are ferromagnetic with the easy axis of magnetization in the film plane at room temperature, indicated by spin polarization of secondary electrons. This is supported by the observation of highly polarized ($P > 50\%$) photoelectrons emitted by the films. The photoemission peaks obtained for normal emission with *s*-polarized light from the (001) surface are shifted by about 0.4 eV to higher binding energy, compared to band-structure calculations on face-centered-cubic Fe with an expanded lattice constant of 7.0 a.u. performed by Bagayoko *et al.*[25] The measured exchange splitting of 2.2 eV at $\Gamma_{25}'$ agrees well with the value predicted by Bagayoko *et al.*[25] Our results indicate that $\gamma$-Fe is a strong ferromagnet.

*Present address: Institut für Angewandte Physik der Heinrich-Heine-Universität Düsseldorf, Universitätsstrasse 1, D-4000 Düsseldorf 1, Germany.

†Present address: Continential A.G., Postfach 169, D-3000 Hannover 1, Germany.

[1]M. Hansen and K. Anderko, *Constitution of Binary Alloys* (McGraw-Hill, New York, 1958).

[2]W. Sucksmith and R. R. Pearce, Proc. R. Soc. London Ser. A **167**, 189 (1938).

[3]J. B. Newkirk, Trans. Metall. Soc. AIME **209**, 1214 (1957).

[4]U. Gradmann, W. Kümmerle, and P. Tillmanns, Thin Solid Films **34**, 249 (1976).

[5]W. A. Jesser and J. W. Matthews, Philos. Mag. **15**, 1097 (1967); *ibid.* **17**, 595 (1968).

[6]W. Kümmerle and U. Gradmann, Solid State Commun. **24**, 33 (1977).

[7]A. Knappworst, Z. Metallkd. **45**, 137 (1954).

[8]U. Gonser, J. Meechan, A. H. Muir, and H. Wiedersich, J.

Appl. Phys. **34**, 2373 (1963).
[9]S. C. Abrahams, L. Guttmann, and J. S. Kasper, Phys. Rev. **127**, 2052 (1962).
[10]C. Rau, C. Schneider, G. Xing, and K. Jamison, Phys. Rev. Lett. **57**, 3221 (1986).
[11]U. Gradmann and P. Tillmanns, Phys. Status Solidi A **539**, (1977).
[12]J. G. Wright, Philos. Mag. **24**, 217 (1971).
[13]W. Keune, R. Halbauer, U. Gonser, J. Lauer, and D. L. Williamson, J. Appl. Phys. **48**, 2976 (1977); J. Magn. Magn. Mater. **6**, 192 (1977).
[14]R. Halbauer and U. Gonser, J. Magn. Magn. Mater. **35**, 55 (1983).
[15]W. Becker, H.-D. Pfannes, and W. Keune, J. Magn. Magn. Mater. **35**, 53 (1983).
[16]W. A. A. Macedo and W. Keune, Phys. Rev. Lett. **61**, 475 (1988).
[17]D. Pescia, M. Stampanoni, G. L. Bona, A. Vaterlaus, R. F. Willis, and F. Meier, Phys. Rev. Lett. **58**, 2126 (1987).
[18]C. Liu, E. R. Moog, and S. D. Bader, Phys. Rev. Lett. **60**, 2422 (1988).
[19]P. A. Montano, G. W. Fernando, B. R. Cooper, E. R. Moog, H. M. Naik, S. D. Bader, Y. C. Lee, Y. N. Darici, H. Min, and J. Marcano, Phys. Rev. Lett. **59**, 1041 (1987).
[20]C. L. Fu and A. J. Freeman, Phys. Rev. B **35**, 925 (1987).
[21]L. Kaufman, E. V. Clougherty, and R. F. Weiss, Acta Metall. **11**, 323 (1963).
[22]R. J. Weiss, Proc. Phys. Soc. London **82**, 281 (1963).
[23]J. Madson, O. K. Andersen, U. K. Poulsen, and O. Jepsen, in *Magnetism and Magnetic Materials-1975*, edited by J. J. Becker, G. H. Lauder, and J. J. Rhyne (AIP, New York, 1976), p. 327.
[24]O. K. Andersen, J. Madsen, U. K. Poulsen, O. Jepsen, and J. Kollar, Physica B+C **86-88B**, 249 (1977).
[25]D. Bagayoko and J. Callaway, Phys. Rev. B **28**, 5419 (1983); D. Bagayoko, doctoral thesis, Louisiana State University, 1983 (unpublished).
[26]V. L. Moruzzi, P. M. Marcus, K. Schwarz, and P. Mohn, Phys. Rev. B **34**, 1784 (1986).
[27]V. L. Moruzzi, Phys. Rev. Lett. **57**, 2211 (1986).
[28]V. L. Moruzzi, P. M. Marcus, and J. Kübler, Phys. Rev. B **39**, 6957 (1989).
[29]H.-O. Isbert and U. Gradmann, J. Magn. Magn. Mater **15-18**, 1109 (1980).
[30]*Pearson's Handbook of Crystallographic Data for Intermetallic Phases* (American Society for Metals, Clevaland, 1985).
[31]S. H. Lu, J. Quinn, D. Tian, F. Jona, and P. M. Marcus, Surf. Sci. **209**, 364 (1989).
[32]J. B. Pendry, *Low Energy Electron Diffraction* (Academic, London, 1974).
[33]A. Amiri Hezaveh, G. Jennings, D. Pescia, R. F. Willis, K. Prince, M. Surman, and A. Bradshaw, Solid State Commun. **57**, 329 (1986).
[34]C. C. Chang, Surf. Sci. **48**, 9 (1975).
[35]M. P. Seah, Surf. Sci. **32**, 703 (1972).
[36]S. A. Chambers, T. J. Wagener, and J. H. Weaver, Phys. Rev. B **36**, 8992 (1987).
[37]S. D. Bader and E. R. Moog, J. Appl. Phys. **61**, 3729 (1987).
[38]M. Landolt, R. Allenspach, and D. Mauri, J. Appl. Phys. **57**, 3626 (1985).
[39]M. Przybylski and U. Gradman, Phys. Rev. Lett. **59**, 1152 (1987).
[40]D. Pescia, G. Zampieri, M. Stampanoni, G. L. Bona, R. F. Willis, and F. Meier, Phys. Rev. Lett. **58**, 933 (1987).
[41]U. Gradmann, Appl. Phys. **3**, 161 (1974).
[42]N. C. Koon, B. T. Jonker, F. A. Volkening, J. J. Krebs, and G. A. Prinz, Phys. Rev. Lett. **59**, 2463 (1987).
[43]B. T. Jonker, K. H. Walker, E. Kisker, G. A. Prinz, and C. Carbone, Phys. Rev. Lett. **57**, 142 (1986).
[44]Z. Q. Wang, S. C. Wu, J. Quinn, C. K. C. Lok, Y. S. Li, and F. Jona, Phys. Rev. B **38**, 7442 (1988).

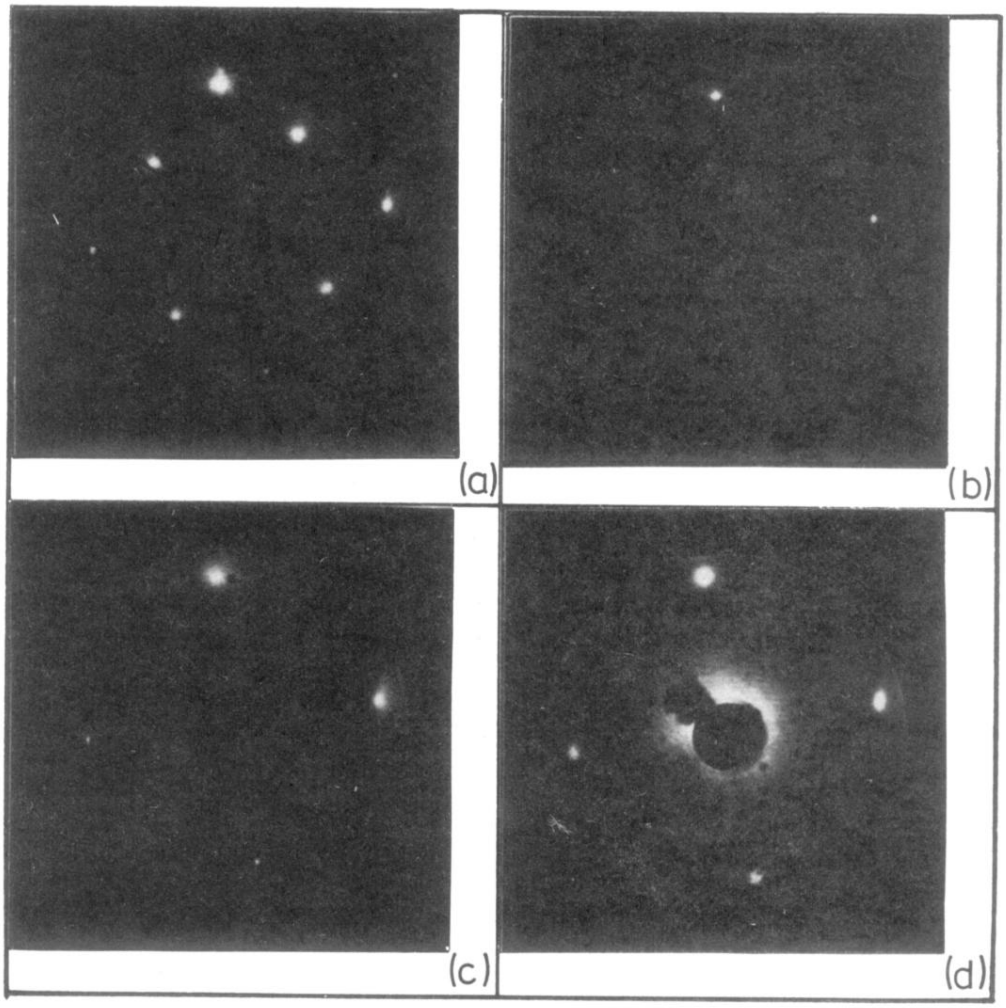


FIG. 1. (a) LEED pattern at 70 eV of a clean and ordered $Cu_3Au(001)$ surface; the four (11) spots are evident. The spots between the (11) spots are due to the superstructure of the ordered alloy. (b) LEED pattern at 70 eV of a clean $Cu_3Au$ surface at $T > 390\,^{\circ}C$: the superstructure spots have vanished. (c) LEED pattern at 70 eV after deposition of 5 ML of Fe: the (11) spots remained at the same position as for $Cu_3Au$. (d) LEED pattern at 55 eV after deposition of 250 ML of Fe: the four (10) spots are evident. The lattice parameter is 2.85 Å.